J. Biochem. 123, 978-983 (1998)

Structure and Distribution of N-Glycans on the S_7-Allele Stylar Self-Incompatibility Ribonuclease of *Nicotiana alata*[1]

David Oxley,*,[2] Sharon L.A. Munro,† David J. Craik,† and Antony Bacic*

*Plant Cell Biology Research Centre, School of Botany, University of Melbourne, Parkville, Victoria 3052, Australia; and †Victorian College of Pharmacy, Parkville, Victoria 3052, Australia

Received for publication, January 7, 1998

S-RNases are the stylar products of the self-incompatibility (S)-locus in solanaceous plants (including *Nicotiana alata*), and as such, are involved in the prevention of self-pollination. All cDNA sequences of S-RNase products of functional S-alleles contain potential N-glycosylation sites, with one site being conserved in all cases, suggesting that N-glycosylation is important in self-incompatibility. In this study, we report on the structure and localization of the N-glycans on the S_7-allele RNase of *N. alata*. A total of nine N-glycans, belonging to the high-mannose- and xylosylated hybrid-classes, were identified and characterized by a combination of electrospray-ionization mass-spectrometry (ESI-MS), ^{1}H-NMR spectroscopy, and methylation analyses. The glycosylation pattern of individual glycosylation sites was determined by ESI-MS of the glycans released from isolated chymotryptic glycopeptides. All three N-glycosylation sites showed microheterogeneity and each had a unique complement of N-glycans. The N-glycosylation pattern of the S_7-RNase is significantly different to those of the S_1- and S_2-RNases.

Key words: N-glycan, microheterogeneity, *Nicotiana alata*, ribonuclease, self-incompatibility.

The self-incompatibility RNases (S-RNases) are an allelic series of glycoproteins produced in the styles of solanaceous plants (including *Nicotiana alata*), which are involved in the rejection of self pollen. It is thought that in an incompatible mating, S-RNase enters the pollen tube and degrades RNA, leading to arrest of pollen tube growth, whereas, in a compatible mating S-RNase is prevented from degrading RNA, *via* interaction(s) with unknown pollen component(s) (for a review, see Refs. *1* and *2*).

As part of our work towards understanding the mechanism of self-incompatibility, we have been examining the structures and distribution of N-glycans on the S-RNases of *N. alata*. Up to five potential N-glycosylation sites (I-V) occur in the S-RNases of *N. alata*, but only the S_3-RNase contains all five sites; the S_2-, S_6- and S_7-RNases each contain four sites (I, II, IV, and V) and the S_1-RNase contains only site I (*3-6*). The single potential N-glycosylation site on the S_1-RNase, which is conserved in all S-RNases of the Solanaceae, is occupied, but the other four *N. alata* S-RNases each have one unoccupied site (*7*). The N-glycans on the S_1- and S_2-RNases are small xylosylated hybrid-types (*8*), whereas the S_3- and S_6-RNases contain a much larger range of N-glycans including high-mannose types (*9*).

We now complete the structural analyses of the N-glycans from the *N. alata* S-RNases with this report on the S_7-RNase and compare the site-specific glycosylation of this protein with those of the S_1- and S_2-RNases.

MATERIALS AND METHODS

Plant Material—Plants of self-incompatibility genotype S_7S_7 were produced as described previously (*3*).

Isolation of S_7-RNase—S_7-RNase was isolated from 100 styles from *N. alata* plants of S-genotype S_7S_7 by a modification of the method of Jahnen *et al.*, (*10*) as described by Oxley and Bacic (*11*). The purity was verified by SDS-PAGE.

Isolation of N-Glycans—Methods for the release of N-glycans from S_7-RNase and their purification by high-pH anion-exchange HPLC were as described previously (*9*).

N-Glycans were released from glycopeptides (see below) by treatment with N-glycanase (0.2 unit) at 37°C for 18 h in 100 mM ammonium bicarbonate (50 μl). The digestion products were applied to the reversed-phase HPLC column and both the released N-glycans (unbound) and deglycosylated peptides were recovered.

Liquid Chromatography—Reversed-phase HPLC was

[1] This work was supported by funds from a Special Research Centre grant from the Australian Research Council. We also acknowledge support for the purchase of the ESI-MS from the Clive and Vera Ramaciotti Foundations, the Ian Potter Foundation, The Australian Research Council and the University of Melbourne.

[2] To whom correspondence should be addressed. Phone: +61-3-9344-5041, Fax: +61-3-9347-1071, E-mail: d.oxley@botany.unimelb.edu.au

Abbreviations: CID, collision induced dissociation; ESI, electrospray-ionization; GlcNAc, 2-acetamido-2-deoxyglucose; Hex, hexose; HexNAc, 2-acetamido-2-deoxyhexose; Man, mannose; MS, mass-spectrometry; NMR, nuclear magnetic resonance; Pent, pentose; Xyl, xylose.

performed on a Brownlee Aquapore RP-300 column (2.1× 130 mm) as described previously (*12*).

Methylation Analysis—Glycans (0.1-1 μg) were methylated by a modification of the procedure of Ciucanu and Kerek (*13*) as described by Oxley and Bacic (*11*). Per-*O*-methylated glycans were either analyzed directly by ESI-MS (see below), or converted to partially methylated alditol acetates and analyzed by GC-MS (*9*).

Chymotrypsin Digestion—Reduction, alkylation, and chymotrypsin digestion of S_7-glycoprotein (100 μg) was performed as described previously except that iodoacetic acid rather than iodoacetamide was used as the alkylating agent (*11*).

Mass-Spectrometry—ESI-MS was performed on a MAT 95 two-sector double focusing mass-spectrometer (Finnigan MAT, Germany) fitted with a Finnigan electrospray source or a Finnigan MAT LCQ. Solvent (0.1% acetic acid in 50% aqueous acetonitrile) was continuously infused into the spectrometer at a flow rate of 4 μl/min using a syringe pump (Harvard Apparatus, USA). Samples (in the same solvent) were injected into the flow stream *via* a Rheodyne injector. MS^n was performed on the LCQ with a 2 mass-unit window for selection of the parent ion and a collision energy of 50%. Data were processed using Finnigan MAT software.

N-Terminal Peptide Sequencing—Peptides were sequenced using a Beckman LF3400 protein sequencer (Beckman Instruments) with on-line analysis on a Beckman System Gold HPLC.

^{1}H-NMR Spectroscopy—^{1}H-NMR spectra were recorded for samples in D_2O (99.996 atom%; Cambridge Isotope Laboratories, UK) at 27 or 37°C at 600 MHz using Bruker AM600 spectrometers. Chemical shifts are expressed in ppm downfield from sodium 4,4-dimethyl-4-silapentane-1-sulphonate, but were actually measured relative to internal acetone at 2.225 ppm.

RESULTS

N-Glycans were released from *N. alata* S_7-RNase using *N*-glycanase. ESI-MS of the total *N*-glycan pool both as native glycans and the per-*O*-methylated derivatives (Table I) indicated the presence of nine *N*-glycans which were fractionated by high-pH anion-exchange HPLC (Fig. 1).

Fraction 1—ESI-MS of fraction **1** (Table I) indicated that it contained two glycans with compositions $Hex_3Pent_1HexNAc_2$ (**1a**) and $Hex_3HexNAc_3$ (**1b**) in the ratio ~1:3. Methylation analysis (Table II) suggested that glycan **1a** contained a terminal Xyl residue linked to O-2 of Man-**3** of a $Man_3GlcNAc_2$ pentasaccharide core, and therefore probably has the structure shown (Scheme 1, **1a**).

Other derivatives detected in the methylation analysis indicated that glycan **1b** contained a terminal GlcNAc residue linked to O-2 of either Man-4 or Man-4′. In order to distinguish between these two possible structures, the per-*O*-methylated glycan was subjected to MS-MS analysis. The pseudomolecular ion at *m/z* 1,417.5 corresponding to $[M + Na]^+$ for glycan **1b**, was collisionally activated and the fragment ions produced were analyzed (Fig. 2). The two largest peaks in the fragment ion spectrum arise from the loss of terminal GlcNAc residues. The fragment ion (*m/z* 1,198.7) corresponding to the loss of the non-reducing terminal Man residue was also present, but in much lower abundance. The ion at *m/z* 953.5 confirms the presence of the non-reducing terminal disaccharide element GlcNAc-Man, but does not indicate which Man residue is substituted. However, the ion at *m/z* 880.5 is diagnostic for GlcNAc-Man substitution at O-3 (or O-2 or O-4) of Man-**3**. This ion can arise from ring cleavage of Man-**3** with the loss of a two carbon fragment (C2-C3, or C3-C4) as described by Reinhold *et al.* (*14*), except that the charge is retained on

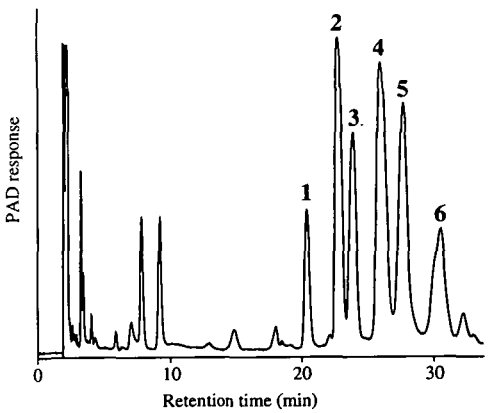

Fig. 1. **Preparative high-pH anion-exchange HPLC chromatogram of the *N*-glycans from *Nicotiana alata* S_7-RNase.** No carbohydrate-containing material was eluted before 20 min. Fractions **1-6** were collected and processed as described in "MATERIALS AND METHODS." As the concentrations of the eluting glycans were outside the linear range of the detector, the relative peak areas are skewed in favor of the glycans of lower abundance. Analytical runs gave relative abundances which were similar to those determined by ESI-MS of the total glycan mixture (Table I).

TABLE I. **ESI-MS of native and per-*O*-methylated *N*-glycans from *N. alata* S_7-RNase.**

	Pseudomolecular ion $[M+Na]^+$				
	Native		Per-*O*-methylated		
Glycan	Calc.	Measured	Calc.	Measured	Composition
1a	1,065.9	1,065.7 (1.3)	1,332.4	1,333.0 (3.0)	$Hex_3Pent_1HexNAc_2$
1b	1,137.0	1,136.9 (4.4)	1,417.5	1,417.2 (6.5)	$Hex_3HexNAc_3$
2	1,269.1	1,268.7 (35.4)	1,577.7	1,577.4 (31.7)	$Hex_3Pent_1HexNAc_3$
3	1,258.1	1,257.7 (10.8)	1,580.7	1,581.1 (13.8)	$Hex_5HexNAc_2$
4a	1,431.2	1,431.7 (27.7)	1,781.9	1,782.0 (22.9)	$Hex_4Pent_1HexNAc_3$
4b	1,472.3	1,471.5 (3.4)	1,823.0	1,823.8 (1.9)	$Hex_3Pent_1HexNAc_4$
5	1,420.2	1,420.9 (11.4)	1,784.9	1,784.1 (14.7)	$Hex_6HexNAc_2$
6a	1,593.4	1,593.5 (1.5)	1,986.1	1,985.8 (0.8)	$Hex_5Pent_1HexNAc_3$
6b	1,582.4	1,582.5 (2.6)	1,989.1	1,988.9 (1.9)	$Hex_7HexNAc_2$

Numbers in parentheses indicate the relative abundance of individual pseudomolecular ions in the spectra of the total *N*-glycan pool.

the reducing fragment. Further support for this assignment was provided by CID-MS of some of the other glycans, the structures of which were deduced by ^{1}H-NMR spectroscopy, *e.g.* glycan **2** which differs from glycan **1b** in that it has a Xyl substituent on O-2 of Man-**3** (see below). This glycan also gave the ion at *m/z* 880.5 arising from the loss of C3-C4 from Man-**3**, as well as an ion at *m/z* 1,040.6 (880.5+Xyl) arising from the loss of C2-C3 (data not shown). Thus, glycan **1b** has the structure shown (Scheme 1, **1b**). Anomeric configurations are inferred from the corresponding glycan from *N. alata* S_6-RNase which was characterized by ^{1}H-NMR spectroscopy (*9*).

Fractions 2, 3, 4, and 5—ESI-MS (Table I) of native and per-*O*-methylated fractions **2**, **3**, **4**, and **5** showed that each contained single major glycans with the compositions $Hex_3Pent_1HexNAc_3$, $Hex_5HexNAc_2$, $Hex_4Pent_1HexNAc_3$, and $Hex_6HexNAc_2$, respectively. In addition to the major glycan (**4a**), fraction **4** contained a single minor glycan (**4b**, ~10%) with the composition $Hex_3Pent_1HexNAc_4$. These

TABLE II. **Methylation analyses of *N. alata* S_7-*N*-glycan fractions from Fig. 1.**

	N-Glycan fraction					
	1	2	3	4	5	6[b]
Residue	Molar proportion					
t-Xyl*p*	0.3	0.6	—	0.8	—	—
t-Man*p*	1.7	1.0	3.3	0.9	4.4	4.3
2-Man*p*	1.2	1.0	—	1.4	1.9	3.1
3-Man*p*	—	—	—	1.2	—	—
3,6-Man*p*	0.8	—	2.0	—	2.5	2.1
2,3,6-Man*p*	0.4	1.1	—	1.1	—	—
t-Glc*p*NAc	0.5	0.8	—	1.0	—	—
4-Glc*p*NAc	2.0	2.0	2.0	2.0	2.0	2.0

—, not detected.

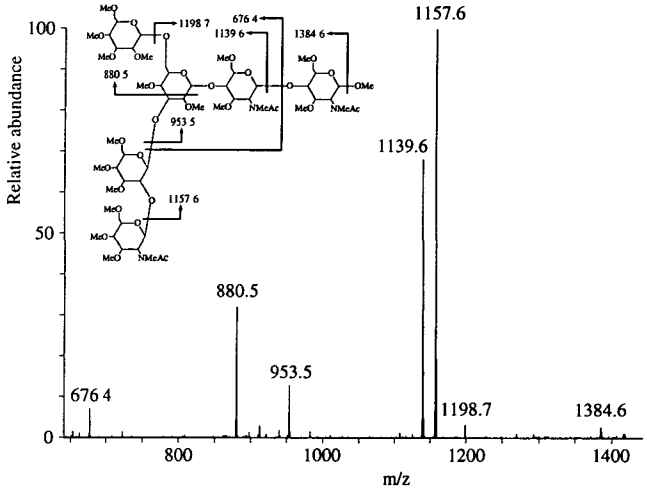

Fig. 2. **MS-MS of the pseudomolecular ion $[M+Na]^+$=1,417.5 of the per-*O*-methylated glycan 1b.**

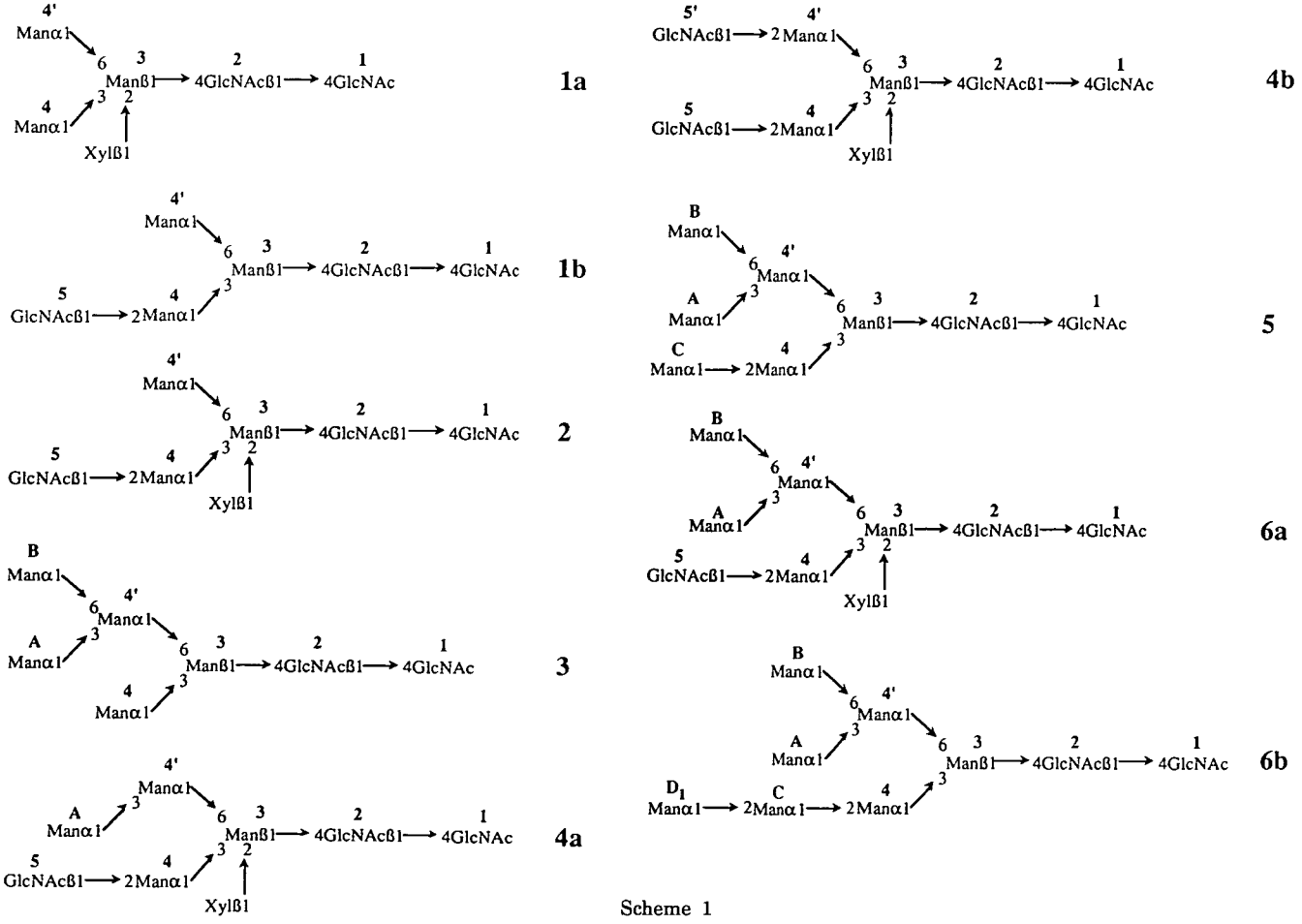

Scheme 1

four fractions were each analyzed by both ^{1}H-NMR spectroscopy and methylation analysis (Table II). Comparison of the ^{1}H-NMR data with reference data (*9, 24*) indicated that glycans **2**, **3**, **4a** and **5** had the structures shown (Scheme **1**, **2**, **3**, **4a**, and **5**). The methylation data (Table II) was consistent with these structures.

Glycan **4b** ($Hex_3Pent_1HexNAc_4$) was further analyzed by MS-MS of the per-*O*-methylated derivative, which showed the presence of fragment ions arising from the loss of reducing- and non-reducing terminal HexNAc and non-reducing terminal Pent residues, but no ions corresponding to loss of terminal Hex residues (data not shown). The most likely structure which fits this data has both Man-4 and Man-4′ substituted by GlcNAc residues, as shown (Scheme 1, **4b**). A glycan with this structure has previously been isolated from *N. alata* S_6-RNase (*9*).

Fraction 6—Fraction **6** was not available in sufficient quantity for NMR analysis. ESI-MS of fraction **6** (Table I) showed the presence of two glycans (**6a** and **6b**) in the ratio ~1:2 with the compositions $Hex_5Pent_1HexNAc_3$ (**6a**) and $Hex_7HexNAc_2$ (**6b**). These two components were separated by rechromatography of fraction **6** by high-pH anion-exchange HPLC with isocratic elution. Methylation analysis of **6b** (Table II) gave derivatives typical of a high-mannose type glycan. MS-MS of the per-*O*-methylated glycan (Fig. 3) showed a series of fragments resulting from the loss of Man_1, Man_2, and Man_3. The presence of the Man_3-loss fragment and the absence of a Man_4-loss fragment clearly demonstrate that both the 3- and 6-antennae carry trimannosyl substituents. Taken together with information on linkage positions and anomeric configurations deduced for the corresponding glycan from the *N. alata* S_6-RNase (*9*), we propose that glycan **6b** has the structure shown (Scheme 1, **6b**).

There was insufficient material for further analysis of glycan **6a**, but based on the monosaccharide composition deduced by ESI-MS and by comparison with the corresponding glycan from *N. alata* S_6-RNase (*9*), it is likely that this glycan has the structure shown (Scheme 1, **6a**).

Chymotrypsin Digestion—Since there are no cleavage sites between the two potential *N*-glycosylation sites I and II for the commonly used specific endoproteases (Lys, Arg, Glu, and Asp), chymotrypsin was used to digest the S_7-RNase. The protein was first reduced and *S*-carboxymethylated to increase the susceptibility to protease digestion. The digestion products were fractionated by reversed-phase HPLC (Fig. 4) and the collected fractions were analyzed by ESI-MS (Table III). Peptides were identified by comparison of their molecular weights with those calculated for every possible peptide deduced from the cDNA sequence (Fig. 5). The peptides identified covered more than 90% of the amino acid sequence including the four potential *N*-glycosylation sites (Fig. 5) and showed that sites I, II, and IV (Asn^{27}, Asn^{37} and Asn^{140}) were glycosylated, while site V (Asn^{152}) was not.

Glycopeptides were readily identified by the presence of series' of ions differing by monosaccharide residue masses

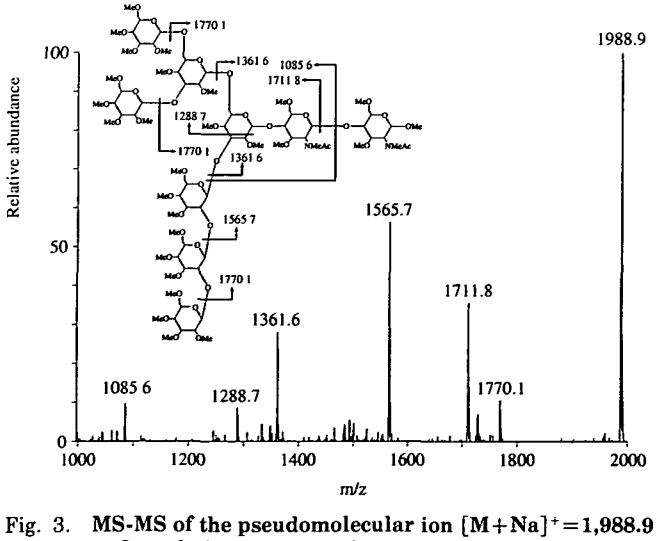

Fig. 3. **MS-MS of the pseudomolecular ion $[M+Na]^+=1,988.9$ of the per-*O*-methylated glycan 6b.**

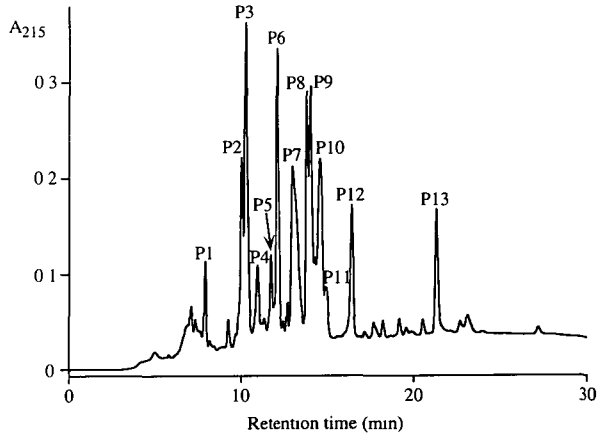

Fig. 4. **RP-HPLC of the chymotrypsin digestion products of reduced and carboxymethylated S_7-RNase.**

TABLE III. **ESI-MS of reduced and carboxymethylated S_7 chymotryptic peptides from Fig. 4.**

Fraction	Molecular weight[a]	Assignment
P1	2,520.6[c]	Thr^{135}-Lys^{144}+$Man_4XylGlcNAc_3$
P2	1,116.6 (a)	Asn^{43}-Phe^{51}
	1,595.7 (b)	Lys^{52}-Tyr^{64}
P3	855.7 (a)	Asn^{100}-Phe^{105}
	2,741.6[b] (b)	Cys^{16}-Phe^{28}+$Man_3GlcNAc_3$
	2,862.6[b] (b)	Cys^{16}-Phe^{28}+$Man_5GlcNAc_2$
	3,024.6[b] (b)	Cys^{16}-Phe^{28}+$Man_6GlcNAc_2$
	3,186.6[b] (b)	Cys^{16}-Phe^{28}+$Man_7GlcNAc_2$
P4	1,206.7	Arg^{122}-Met^{132}
P5	1,493.7	Ser^{119}-Met^{132}
P6	1,147.5	Cys^{77}-Trp^{84}
P7	1,479.7	Lys^{65}-Tyr^{76}
P8	3,100.2	Asp^{170}-Pro^{196}
P9	748.3 (a)	Gln^{10}-Phe^{15}
	2,429.4[c] (b)	Gly^{32}-Leu^{42}+$Man_3XylGlcNAc_3$
P10	900.5 (a)	Ala^{1}-Leu^{7}
	1,285.6 (b)	Asn^{100}-Met^{109}
	2,780.8[c] (c)	Thr^{29}-Leu^{42}+$Man_3XylGlcNAc_3$
P11	1,061.6	Ala^{110}-Leu^{118}
P12	960.5	Val^{8}-Phe^{15}
P13	2,873.0	Lys^{145}-Phe^{169}

[a]Some fractions contained more than one peptide, these are labeled a, b, or c. [b]Peptide P3b gave multiple pseudomolecular ions due to the presence of several abundant *N*-glycans. [c]Only the most abundant glycoform of peptides P1, P9b, and P10c are shown.

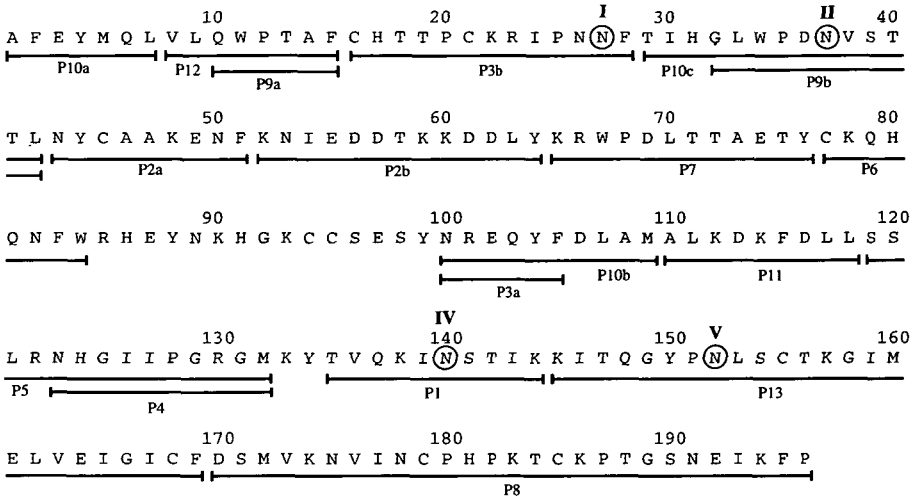

Fig. 5. **The amino acid sequence of the S_7-RNase predicted from the cDNA sequence and location of chymotryptic (glyco)peptides from Fig. 4.** Potential *N*-glycosylation sites are identified by circled Asn residues and are numbered above the Asn residue in Roman numerals.

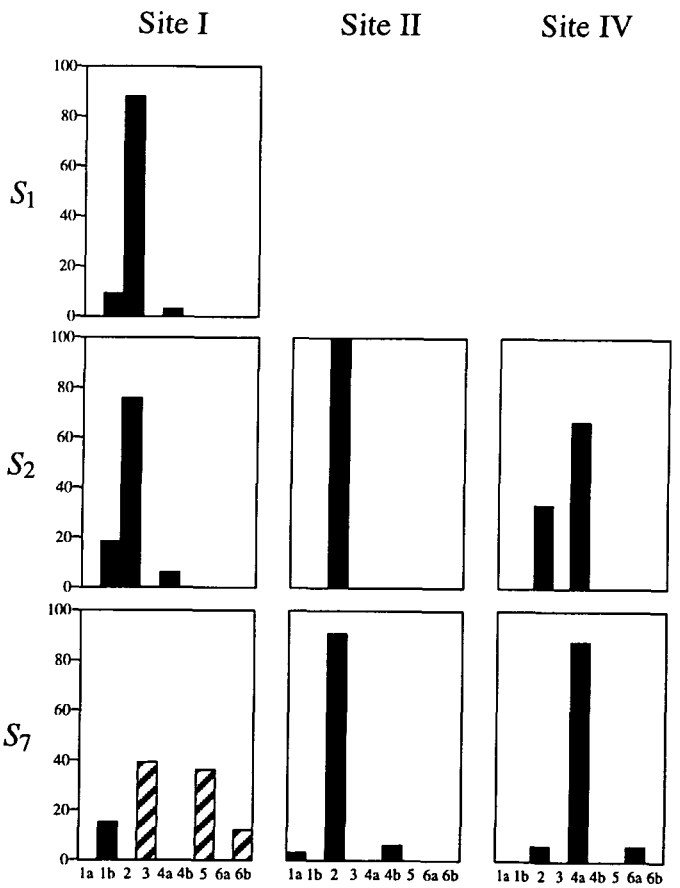

Fig. 6. **Comparison of the *N*-glycan distribution on the S_1- (*7*), S_2- (*11*), and S_7- (this study) RNases of *N. alata*.**

(203 mass units, GlcNAc; 162 mass units, Man; 132 mass units, Xyl). In fact significant fragmentation of the glycan side-chains was evident in all of the glycopeptides, with fragment ion series' extending down to the peptide backbone (*i.e.* cleavage of the GlcNAc–Asn linkage). Since these fragment ions are indistinguishable from genuine pseudomolecular ions, it was not possible to estimate the glycan populations directly by ESI-MS of the glycopeptides. Therefore, glycopeptide fractions P1, P3, and P10, containing the *N*-glycosylation sites IV, I, and II, respectively (Table III), were treated with *N*-glycanase and both the released *N*-glycans and the *N*-deglycosylated peptides were recovered. The molecular weights of the *N*-deglycosylated peptides (determined by ESI-MS) were in agreement with the predicted values (Fig. 5).

The three *N*-glycan pools were per-*O*-methylated and analysed and quantified by ESI-MS (Fig. 6). This showed that there was extensive heterogeneity at *N*-glycosylation site I, which contained all of the high-mannose type glycans (**3**, **5**, and **6b**) as well as glycan **1b** ($Man_3GlcNAc_3$), whereas *N*-glycosylation at sites II and IV consisted almost exclusively of single glycans (**2** and **4a**, respectively).

DISCUSSION

A total of nine *N*-glycans have been identified on the *N. alata* S_7-RNase, with four (**2**, **3**, **4a**, and **5**) accounting for around 85% of the total. These glycans are typical of those found on other plant glycoproteins (*e.g.* Refs. *15–17*), although the lack of any core fucosylation is notable. The range of *N*-glycans on the S_7-RNase is similar to those of the *N. alata* S_3- and S_6-RNases (*9*), but is much more extensive than those of the S_1- and S_2-RNases (*8*) both of which carried only the four glycans $Man_3Xyl_1GlcNAc_2$, $Man_3GlcNAc_3$, $Man_3Xyl_1GlcNAc_3$, and $Man_4Xyl_1GlcNAc_3$ (**1a**, **1b**, **2**, and **4a**). Thus, the five *N. alata* *S*-RNases can be divided into two groups based on their total *N*-glycan profiles, however, no such grouping can be seen based on amino acid sequence similarity (*18*).

It is interesting to compare the site-specific distribution of glycans between members of these two groups (Fig. 6). The site-specific *N*-glycosylation is known for the S_1-RNase [by default, since this protein contains only one *N*-glycosylation site; (*8*)] and for the S_2-RNase (*11*). The only *N*-glycosylation site common to these two *S*-RNases (site I) is similarly glycosylated in both cases (Fig. 6), predominantly with $Man_3Xyl_1GlcNAc_3$ (glycan **2**). However, in the S_7-RNase site I has a completely different glycan profile (Fig. 6) consisting of the high-mannose type *N*-glycans (**3**, **5**, and **6b**) and the hybrid type *N*-glycan $Man_3GlcNAc_3$ (**1b**). Site II in both the S_2- and S_7-RNases

have very similar glycan compositions (Fig. 6) comprising almost exclusively $Man_3Xyl_1GlcNAc_3$ (glycan **2**). The glycan $Man_4Xyl_1GlcNAc_3$ (**4a**) is the major substituent of site IV in both proteins (Fig. 6), although in the S_2-RNase this is accompanied by a significant amount of $Man_3Xyl_1GlcNAc_3$ (glycan **2**). Neither protein is glycosylated at site V. A remarkable feature of the S_7-RNase *N*-glycosylation pattern is the almost complete segregation of the glycans. With the exception of a small amount of glycan **3** at site IV, each glycan is unique to a single glycosylation site (Fig. 6).

The most striking difference in the glycosylation patterns of the S_2- and S_7-RNases is at site I. The presence of high-mannose type glycans at site I in the S_7-RNase is indicative of incomplete processing, which is considered to be due to restricted accessibility of the glycan to the processing enzymes of the Golgi (*19, 20*). This may result from large- or small-scale differences in protein conformation. However, the *S*-RNases are expected to have very similar secondary and tertiary structure, thus, it is more likely that the difference in the glycan processing at site I of the S_2- and S_7-RNases is due to local structural variation. Site I occurs just prior to a conserved β-strand which carries several catalytically important residues (*21*) and would not be expected to show any significant conformational variation. However, it is preceded by a highly variable flexible loop of fourteen amino acids which may be the determining factor.

The role (if any) of the *N*-glycans on the *S*-RNases is still unknown. All cDNA sequences of *S*-RNase products of functional *S*-alleles contain at least one potential *N*-glycosylation site, with site I being conserved in all cases. However, this site is not present on the *S*-like RNases, which are not involved in self-incompatibility (*22*), suggesting that glycosylation at least at site I of the *S*-RNases is important in self-incompatibility. It seems that glycosylation of *S*-RNases is not required for correct folding of the proteins since mutagenized *S*-RNase lacking potential *N*-glycosylation sites has been expressed in transgenic plants and retains full RNase activity (*23*). The same study also suggested that *N*-glycosylation is not required for the operation of self-incompatibility, but this has yet to be proven. Further work with transgenic plants will be required to answer this question.

We wish to thank Professor A.E. Clarke for her enthusiasm for this project and for helpful discussions and Dr. Ed Newbigin for helpful suggestions during the preparation of this manuscript.

REFERENCES

1. de Nettancourt, D. (1977) *Incompatibility in Angiosperms*, Springer-Verlag, Berlin
2. Clarke, A.E. and Newbigin, E., (1993) Molecular aspects of self-incompatibility in flowering plants. *Annu. Rev. Genet.* **27**, 257-279
3. Anderson, M.A., Cornish, E.C., Mau, S.-L., Williams, E.G., Hoggart, R., Atkinson, A., Bonig, I., Grego, B., Simpson, R.J., Roche, P.J., Haley, J.D., Penschow, J.D., Niall, H.D., Tregear, G.W., Coghlan, J.P., Crawford, R.J., and Clarke, A.E., (1986) Cloning of cDNA for a stylar glycoprotein associated with expression of self-incompatibility in *Nicotiana alata*. *Nature* **321**, 38-44
4. Anderson, M.A., McFadden, G.I., Bernatzky, R., Atkinson, A., Orpin, T., Dedman, H., Tregear, G., Fernley, R., and Clarke, A.E. (1989) Sequence variability of three alleles of the self-incompatibility gene of *Nicotiana alata*. *Plant Cell* **1**, 483-491
5. Kheyr-Pour, A., Bintrim, S.B., Ioerger, T.R., Remy, R., Hammond, S.A. and Kao, T.-H. (1990) Sequence diversity of pistil *S*-proteins associated with gametophytic self-incompatibility in *Nicotiana alata*. *Sex. Plant Reprod.* **3**, 88-97
6. Vissers, A., Dodds, P., Golz, J.F., and Clarke, A.E. (1995) Cloning and nucleotide sequence of the S_7 RNase from *Nicotiana alata* Link and Otto. *Plant Physiol.* **108**, 427-428
7. Woodward, J.R., Bacic, A., Jahnen, W., and Clarke, A.E. (1989) N-linked glycan chains on *S*-allele-associated glycoproteins from *Nicotiana alata*. *Plant Cell* **1**, 511-514
8. Woodward, J.R., Craik, D., Dell, A., Khoo, K.-H., Munro, S.L.A., Clarke, A.E., and Bacic, A. (1992) Structural analysis of the N-linked glycan chains from a stylar glycoprotein associated with expression of self-incompatibility in *Nicotiana alata*. *Glycobiology* **2**, 241-250
9. Oxley, D., Munro, S.L.A., Craik, D.J., and Bacic, A. (1996) Structure of the *N*-glycans on the S_3- and S_6-allele stylar self-incompatibility ribonucleases of *Nicotiana alata*. *Glycobiology* **6**, 611-618
10. Jahnen, W., Batterman, M.P., Clarke, A.E., Moritz, R.L., and Simpson, R.J. (1989) Identification, isolation and N-terminal sequencing of style glycoproteins associated with self-incompatibility in *Nicotiana alata*. *Plant Cell* **1**, 493-499
11. Oxley, D. and Bacic, A. (1995) Microheterogeneity of N-glycosylation on a stylar self-incompatibility glycoprotein of *Nicotiana alata*. *Glycobiology* **5**, 517-523
12. Oxley, D. and Bacic, A. (1996) Disulphide bonding in a stylar self incompatibility ribonuclease of *Nicotiana alata*. *Eur. J. Biochem.* **242**, 75-80
13. Ciucanu, I. and Kerek, F. (1984) A simple and rapid method for the permethylation of carbohydrates. *Carbohydr. Res.* **131**, 209-217
14. Reinhold, V.N., Reinhold, B.B. and Chan, S. (1996) Carbohydrate sequence analysis by electrospray ionization-mass spectrometry. *Methods Enzymol.* **271**, 377-402
15. Hayashi, M., Tsuru, A., Mitsui, T., Takahashi, N., Hanzawa, H., Arata, Y., and Akazawa, T. (1990) Structure and biosynthesis of the xylose-containing carbohydrate moeity of rice α-amylase. *Eur. J. Biochem.* **191**, 287-295
16. Sturm, A. (1991) Heterogeneity of the complex N-linked oligosaccharides at specific glycosylation sites of two secreted carrot glycoproteins. *Eur. J. Biochem.* **199**, 169-179
17. Gray, J.S.S., Yang, B.Y., Hul, S.R., Venzke, D.P., and Montgomery, R. (1996) The glycans of soybean peroxidase. *Glycobiology* **6**, 23-32
18. Haring, V.H., McClure, B.A., and Clarke, A.E. (1991) Molecular aspects of self-incompatibility in the solanacae in *Advances in Plant Gene Research* (Dennis, E. and Llewellyn, D., eds.) Vol. 7, pp. 149-160, "Molecular approaches to crop improvement," Springer-Verlag, Vienna
19. Faye, L., Sturm, A., Bollini, R., Vitale, A., and Chrispeels, M.J. (1986) The position of the oligosaccharide side-chains of phytohemagglutinin and their accessibility to glycosidases determines their subsequent processing in the Golgi. *Eur. J. Biochem.* **158**, 655-661
20. Ashford, D.A., Alafi, C.D., Gamble, V.M., Mackay, D.J.G., Rademacher, T.W., Williams, P.J., Dwek, R.A., Barclay, A.N., Davis, S.J., Somoza, C., Ward, H.A., and Williams, A.F. (1993) Site-specific glycosylation of recombinant rat and human soluble CD4 variants expressed in chinese hamster ovary cells. *J. Biol. Chem.* **268**, 3260-3267
21. Parry, S.K., Newbigin, E., Craik, D., Nakamura, K., Bacic, A., and Oxley, D. (1998) Structural analysis and molecular model of a self-incompatibility RNase from wild tomato. *Plant Physiol.* **116**, 463-469
22. Green, P.J. (1994) The ribonucleases of higher plants. *Plant Physiol. Plant Mol. Biol.* **45**, 421-445
23. Karunanandaa, B., Huang, S., and Kao, T.-H. (1994) Carbohydrate moiety of the *Petunia inflata* S_3-protein is not required for self-incompatibility interactions between pollen and pistil. *Plant Cell* **6**, 1933-1940
24. Fu, D., Chen, L., and O'Neill, R.A. (1994) A detailed structural characterization of ribonuclease B oligosaccharides by ^{1}H-NMR spectroscopy and mass spectrometry. *Carbohydr. Res.* **261**, 173-186